Cell, Vol. 82, 545–554, August 25, 1995, Copyright © 1995 by Cell Press

Group II Intron Mobility Occurs by Target DNA-Primed Reverse Transcription

Steven Zimmerly,* Huatao Guo,* Philip S. Perlman,† and Alan M. Lambowitz*
*Departments of Molecular Genetics, Biochemistry, and Medical Biochemistry
The Ohio State University
Columbus, Ohio 43210-1292
†Department of Biochemistry
University of Texas Southwestern Medical Center
Dallas, Texas 75235-9038

Summary

Mobile group II introns encode reverse transcriptases and insert site specifically into intronless alleles (homing). Here, in vitro experiments show that homing of the yeast mtDNA group II intron al2 occurs by reverse transcription at a double-strand break in the recipient DNA. A site-specific endonuclease cleaves the antisense strand of recipient DNA at position +10 of exon 3 and the sense strand at the intron insertion site. Reverse transcription of al2-containing pre-mRNA is primed by the antisense strand cleaved in exon 3 and results in cotransfer of the intron and flanking exon sequences. Remarkably, the DNA endonuclease that initiates homing requires both the al2 reverse transcriptase protein and al2 RNA. Parallels in their reverse transcription mechanisms raise the possibility that mobile group II introns were ancestors of nuclear non-long terminal repeat retrotransposons and telomerases.

Introduction

Group II introns are highly structured, catalytic RNAs that splice via a lariat intermediate and are believed to be related to the progenitors of spliceosomal introns (see Michel et al., 1989; Saldanha et al., 1993). Consistent with an early evolutionary origin, group II introns have been found in bacteria and in mitochondria and chloroplasts, organelles that evolved from endosymbiotic bacteria (Michel et al., 1989; Ferat and Michel, 1993). In one scenario, group II introns associated with organelles in early eukaryotes migrated to the nucleus where their structural and catalytic domains evolved into *trans*-acting snRNAs (Cavalier-Smith, 1991; Palmer and Logsdon, 1991). Remarkably, some group II introns encode reverse transcriptases (RTs) and propagate as mobile genetic elements (see Lambowitz and Belfort, 1993). The existence of such mobile group II introns suggests an evolutionary relationship between introns and retroelements and may have implications for the dispersal of introns in eukaryotic genomes.

The best characterized mobile group II introns are introns 1 and 2 of the *COX1* gene of yeast mtDNA (denoted al1 and al2). Each of these introns encodes an open reading frame (ORF) that is translated in-frame with the upstream exon and then processed to give an active intron-encoded protein (Carignani et al., 1983; Moran et al., 1994). Like other group II intron-encoded proteins, the al1 and al2 proteins contain a RT domain, as well as additional conserved domains Z and X, and a C-terminal Zn^{2+} finger–like region (Zn domain; Michel and Lang, 1985; Doolittle et al., 1989; Mohr et al., 1993). Genetic analyses showed that the al1 and al2 proteins are maturases that function specifically in splicing the intron in which they are encoded (Carignani et al., 1983; Moran et al., 1994), and biochemical studies showed that these proteins are also active RTs (Kennell et al., 1993). In mitochondrial ribonucleoprotein (mtRNP) particle preparations, the al2 RT preferentially reverse transcribes al2-containing RNAs and initiates cDNA synthesis near the 3′ end of al2 and nearby in exon 3 of the unspliced pre-mRNA. The maturase function of the al2 protein presumably reflects that its specific binding to the intron RNA, the preferred template for reverse transcription, promotes formation of the catalytically active RNA structure (Kennell et al., 1993).

Both al1 and al2 are mobile elements that insert efficiently and site specifically into intronless alleles during crosses (Meunier et al., 1990; Lazowska et al., 1994; Moran et al., 1995), and al1 has also been shown to transpose to ectopic sites at low frequency (Mueller et al., 1993). The site-specific insertion of the intron, referred to as homing, is a duplicative transposition. It does not generate target site repeats, but is accompanied by coconversion of flanking exon sequences (Lazowska et al., 1994; Moran et al., 1995). Although some al1 and al2 alleles home independently, the al1 allele in our wild-type strains does not encode an active RT and is transferred in standard crosses only in association with al2 (Moran et al., 1995). The extent of coconversion and the cotransfer of al1 and al2 in crosses in which al1 is not independently mobile suggest that the mobility intermediate is a reverse transcript of unspliced *COX1* pre-mRNA that begins in exon 3 and extends through the intron into exon 1 (Kennell et al., 1993; Lazowska et al., 1994; Moran et al., 1995).

Analysis of al2 mutants indicated that homing involves both the RT activity of the al2 protein and a second activity that is associated with the Zn domain (Moran et al., 1995). The latter activity was inferred from the analysis of a Zn domain mutant, $1^{0}2^{P714T}$, which has elevated endogenous RT activity with al2-containing RNA templates, but is nevertheless strongly deficient in al2 mobility. Notably, the Zn domains of group II intron proteins contain two conserved sequences, E-X_1-H-H and H-X_3-H, that are characteristic of a family of DNases (Gorbalenya, 1994; Shub et al., 1994). A requirement for a site-specific DNA endonuclease in group II intron mobility was also suggested by the finding that homing of al1 is impeded by sequence changes in the recipient allele in interspecies crosses (Lazowska et al., 1994).

There have also been indications that group II intron homing is dependent on the splicing or structure of the

intron RNA (Meunier et al., 1990; Moran et al., 1995). The best evidence for such involvement comes from analysis of the mutant $1^{+}2^{\Delta D5}$, which does not splice al2 because of the deletion of intron domain V. This mutant continues to synthesize active al2 RT, but is completely deficient in mobility (Moran et al., 1995).

Retroelements can be divided into two major classes, depending on whether or not their replicative forms contain long terminal repeats (LTRs). Amino acid sequence alignments indicate that the group II intron RTs are related to those encoded by the non-LTR retroelements, a diverse group that includes the abundant human LINE elements (Doolittle et al., 1989; Xiong and Eickbush, 1990; Eickbush, 1994). It has been suggested that non-LTR elements retrotranspose by using the 3′ OH of a nicked genomic DNA strand to prime reverse transcription at the 3′ end of the RNA of the element (reviewed by Eickbush, 1992). This mechanism, referred to as target DNA–primed reverse transcription, has been demonstrated biochemically for the Bombyx mori R2 element (R2Bm; Luan et al., 1993). Although many non-LTR retrotransposons insert nonspecifically and may use random nicks for priming, the R2Bm RT generates the initial break by cleaving site specifically at the preferred insertion site in the 28S rRNA gene. Interestingly, the R2Bm-encoded protein by itself nicks one strand of the target DNA, but requires an RNA cofactor to make a double-strand break (Luan et al., 1993).

Here, we used an in vitro system to show that the retrotransposition of the yeast mtDNA group II intron al2 occurs by an analogous target DNA–primed reverse transcription mechanism that results in cotransfer of the intron and flanking exon sequences. Remarkably, our results provide evidence that the DNA endonuclease activity that cleaves the recipient DNA requires not only the al2 RT protein, but also the intact intron RNA, which could function as a cofactor or catalytic component. Parallels in their reverse transcription mechanisms raise the possibility that mobile group II introns were not only progenitors of nuclear pre-mRNA introns, but also of nuclear non-LTR retrotransposons and telomerases.

Results

Detection of Putative Mobility Intermediates In Vitro

To reconstitute the intron homing reaction in vitro, mtRNP particles from intron donor strains were incubated with a target plasmid that contains the intron homing site (i.e., ligated exons 2 and 3) in the presence of [^{32}P]dCTP and other dNTPs. We reasoned that mobility products or intermediates might be detected as labeled forms of the plasmid that contain products of al2 reverse transcription joined to the homing site. Figure 1 shows that plasmid-dependent labeled bands (marked by asterisks) were observed after incubation of plasmid pJVM159 with mtRNP particles from the wild-type $1^{+}2^{+}$ strain and $1^{0}2^{+t}$, a strain that lacks al1 but contains a mobility-competent al2 (see Figure 2 for plasmid map and Experimental Procedures for nomenclature of *COX1* alleles). Assays with these strains

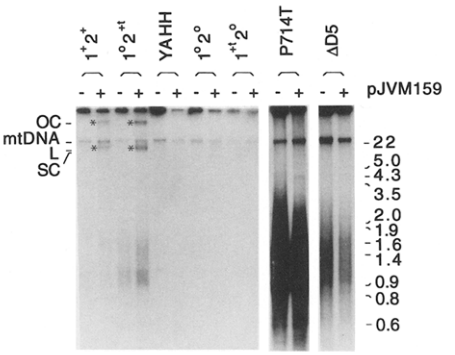

Figure 1. Synthesis of Putative al2 Mobility Products In Vitro

mtRNP particles (0.025 U, OD_{260}) from various yeast strains were incubated with (plus) or without (minus) 1 μg of plasmid pJVM159 in 100 mM KCl, 2 mM $MgCl_2$, 50 mM Tris–HCl (pH 8.5), 5 mM DTT, and [^{32}P]dCTP plus other dNTPs, as described in Experimental Procedures. The products were analyzed by electrophoresis in a nondenaturing 1% agarose gel, followed by autoradiography. Strains were wild-type 161 ($1^{+}2^{+}$), $1^{0}2^{+t}$, $1^{0}2^{YAHH}$ (YAHH), $1^{0}2^{0}$, $1^{+t}2^{0}$, $1^{0}2^{P714T}$ (P714T), and $1^{+}2^{\Delta D5}$ (ΔD5). All samples were run in parallel on the same gel. The plasmid-dependent labeled bands in $1^{+}2^{+}$ and $1^{0}2^{+t}$ are indicated by asterisks. OC, L, and SC indicate positions of open circular, linear, and supercoiled forms of the plasmid DNA detected by ethidium bromide staining. Numbers to the right indicate sizes (in kilobases) of EcoRI–HindIII fragments of phage λ DNA used as size markers.

generally gave two major plasmid-dependent bands, as well as lighter bands, with some variation in the relative intensities of the bands with different reaction conditions and mtRNP particle preparations (see below). By contrast, plasmid-dependent labeled bands were not detected with mtRNP particles from the $1^{0}2^{0}$ and $1^{+t}2^{0}$ strains, which lack al2, or with the $1^{0}2^{YAHH}$ mutant, which has a mutation in the conserved YADD motif of the al2 protein that eliminates RT activity. We show below that the plasmid-dependent labeled bands result from the incorporation of cDNAs into the recipient plasmid. Additionally, all of the strains showed some labeling of the mtDNA, presumably by the mtDNA polymerase, and strains having active al2 RT show heterogeneous cDNAs (0.6–3.5 kb size markers) that were synthesized from endogenous RNP particle templates independently of the target plasmid (see Kennell et al., 1993). Other experiments confirmed that synthesis of the plasmid-dependent labeled bands requires all four dNTPs and is inhibited by digesting the RNP particles with RNase A (data not shown), as expected for reverse transcription using an RNA template. In addition, the extent of labeling was equal for circular or linearized plasmid, and the reaction was inhibited in the presence of EDTA or proteinase K (data not shown).

Analysis of two additional mutants showed that synthesis of the ^{32}P-labeled plasmid bands is correlated with the mobility phenotypes of the strains. First, mtRNP particles from the mobility-deficient Zn domain mutant $1^{0}2^{P714T}$ synthesize little if any of the labeled plasmid products seen in the wild-type $1^{+}2^{+}$ or $1^{0}2^{+t}$ strains, even though the mutant overproduces ^{32}P-labeled cDNAs from endogenous RNA templates (see Kennell et al., 1993). In the experiment of

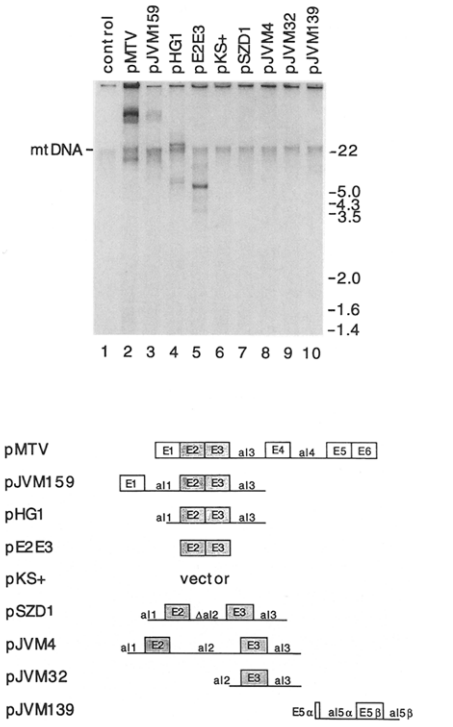

Figure 2. ^{32}P Labeling of the Target Plasmid Requires the Intron Homing Site

Various plasmid DNAs (1 μg) were incubated with wild-type $1^{+}2^{+}$ mtRNP particles for the synthesis of ^{32}P-labeled cDNAs as in Figure 1, except that the reaction medium was at pH 7.5 and contained 5 mM $MgCl_2$. Products were analyzed by electrophoresis in a 1% agarose gel, followed by autoradiography. Lane 1, control, RNP particles incubated without added plasmid; lanes 2–5, plasmids containing the al2 homing site (pMTV, pJVM159, pHG1, and pE2E3); lane 6, vector pBluescript KS(+) (pKS+); lanes 7 and 8, plasmids having the al2 donor configuration of the *COX1* gene (pSZD1 and pJVM4); lanes 9 and 10, plasmids containing downstream regions of the *COX1* gene (pJVM32 and pJVM139). Numbers to the right indicate sizes (in kilobases) of EcoRI–HindIII fragments of phage λ DNA. The schematics below depict the intron and exon composition of the plasmid inserts (not drawn to scale). Exons 2 and 3 are stippled.

Figure 1, the mutant did appear to synthesize a faster-migrating plasmid-dependent band, but this band was not observed reproducibly. Likewise, mtRNP particles from the splicing-defective mutant $1^{+}2^{\Delta D5}$, which is deficient in mobility and also has elevated endogenous RT activity, showed no labeled plasmid bands. Together, these findings indicate that the plasmid-labeling reaction is dependent not only on the RT activity of the al2-encoded protein, but also on one or more additional activities that are impaired in the $1^{0}2^{P714T}$ and $1^{+}2^{\Delta D5}$ mutants.

The Synthesis of Putative Mobility Intermediates Requires the al2 Homing Site

If the synthesis of the plasmid-dependent labeled bands is relevant to intron homing, then it should be specific for plasmids that contain the intron homing site. Confirming this prediction, Figure 2 shows that the labeling activity was detected only with plasmids that contain the al2 homing site (i.e., ligated exons 2 and 3; lanes 2–5), and not with plasmids that contain the corresponding segment of the al2 donor allele (lanes 7 and 8), or other segments of the *COX1* gene (lanes 9 and 10). Notably, plasmid pE2E3, which contains a 71 bp insert encompassing the E2–E3 junction, was labeled (Figure 2, lane 5), whereas the vector without this insert was not labeled (lane 6).

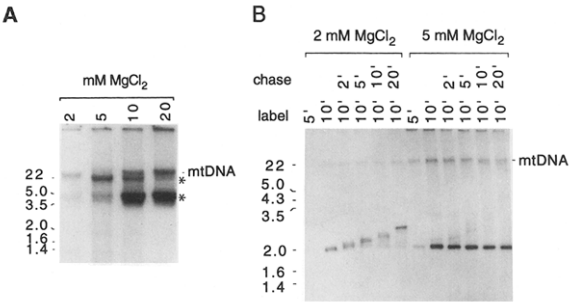

Figure 3. cDNA Synthesis under Different Reaction Conditions

(A) The effect of Mg^{2+} concentration on the pattern of ^{32}P-labeled plasmid products. Wild-type $1^{+}2^{+}$ mtRNP particles were incubated with pE2E3 for the synthesis of ^{32}P-labeled cDNAs in reaction medium at pH 7.5 containing 2, 5, 10, or 20 mM $MgCl_2$. The products were analyzed by electrophoresis in a 1% agarose gel, followed by autoradiography. The predominant plasmid-dependent labeled bands are indicated by asterisks.

(B) Time course showing the effect of Mg^{2+} concentration on the processivity of DNA polymerization. Target plasmid pE2E3 was incubated with wild-type $1^{+}2^{+}$ mtRNP particles in the presence of [^{32}P]dCTP plus other dNTPs in a 6-fold scaled-up reaction at pH 7.5 with 2 or 5 mM $MgCl_2$. After 10 min, the reaction was chased with 0.2 mM dCTP. At the times indicated in the Figure, the products were extracted with phenol–CIA, digested with ScaI and RNase A (see Experimental Procedures), and analyzed by electrophoresis in a 1% agarose gel, followed by autoradiography. In both panels, the numbers at the left indicate sizes (in kilobases) of EcoRI–HindIII fragments of phage λ DNA.

Analysis of cDNA Products Synthesized under Different Reaction Conditions

Initial experiments used the standard RT reaction medium containing 2 mM Mg^{2+}. As shown in Figure 3A, the intensities of the labeled plasmid bands (asterisks) increased at higher Mg^{2+} concentrations, but the distribution of products shifted toward faster migrating species. Subsequent experiments revealed that polymerization is more processive at 2 mM Mg^{2+}, but the DNA endonuclease required to initiate cDNA synthesis is more active at higher Mg^{2+} (see below). The processivity difference is illustrated by the time course in Figure 3B, in which the ^{32}P-labeled plasmid products were digested with RNase A to remove template RNA and then linearized with ScaI and analyzed by gel electrophoresis. At 2 mM Mg^{2+}, the ^{32}P-labeled products increased progressively in size, as expected for the synthesis of cDNAs joined to the plasmid, whereas the products synthesized at higher Mg^{2+} (5 mM or greater) did not increase similarly in size. Denaturing gel electrophoresis showed that polymerization at 2 mM Mg^{2+} extended for at least 400 nt after 20 min at 37°C (data not shown). By contrast, cDNAs synthesized at higher Mg^{2+} concentra-

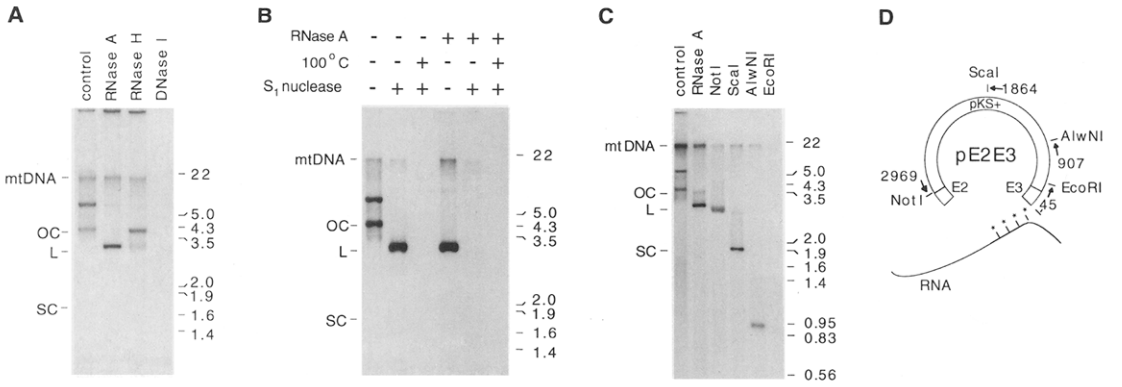

Figure 4. Structure of ^{32}P-Labeled Plasmid Products Analyzed by Nuclease Digestion

^{32}P-labeled products were synthesized with wild-type 1^+2^+ mtRNP particles and recipient plasmid pE2E3 at 5 mM $MgCl_2$ and pH 7.5. The products were digested with various nucleases, as described in Experimental Procedures, and analyzed by electrophoresis in 1% agarose gels, followed by autoradiography. Numbers to the right indicate sizes (kilobases) of EcoRI–HindIII fragments of phage λ DNA. In (A), ^{32}P-labeled products from a 4-fold scaled-up reaction were divided into four parts and either untreated (control) or digested with RNase A, RNase H, or DNase I. In (B), ^{32}P-labeled products from a 6-fold scaled-up reaction were split into six parts and digested with S_1 nuclease with or without prior RNase A treatment. The indicated samples were heated to 100°C for 5 min prior to S_1 nuclease digestion. In (C), ^{32}P-labeled products from a 6-fold scaled-up reaction were divided into six parts and either left untreated, digested with RNase A, or digested with RNase A plus the indicated restriction enzyme. The small labeled EcoRI fragment is not detectable in agarose gels, but was detected in polyacrylamide gels. (D) shows the inferred structure of the ^{32}P-labeled plasmid products and the cleavage sites corresponding to the restriction enzymes used in (C).

tions were found to be truncated at a discrete site within the intron (see below). After further optimization (see Experimental Procedures), we developed two standard reaction media: one at 2 mM Mg^{2+} and pH 8.5 for experiments requiring synthesis of elongated cDNA products and the other at higher Mg^{2+} and pH 7.5 for experiments requiring maximum labeling or cleavage of the recipient plasmid.

Characterization of the ^{32}P-Labeled Plasmid Bands by Nuclease Digestion

The above results suggested that the ^{32}P-labeled plasmid bands arise from reverse transcription primed by the target DNA, analogous to the mechanism used by the R2Bm element (Luan et al., 1993). This process is expected to involve a structure similar to that shown in Figure 4D, in which ^{32}P-labeled cDNAs are incorporated at the site of a nick or double-strand break in the plasmid DNA. To test this model, the ^{32}P-labeled plasmid products synthesized with pE2E3 and 1^+2^+ mtRNP particles were digested with various nucleases. As shown in Figure 4A, RNase A digestion, carried out under low salt conditions to degrade both single-stranded and duplexed RNA, reduced most of the ^{32}P-labeled products to a single predominant band, which migrated close to linear pE2E3 detected by ethidium bromide staining. The reduction in size is expected for removal of the RNA template, and the migration near linear plasmid suggests that the labeled plasmid has a double-strand break. Significantly, the finding that the RNase A digestion reduced the products to a single predominant band indicates that the initial size heterogeneity reflects different-sized RNAs (e.g., differentially processed forms of *COX1* precursor RNA) associated with the target plasmid.

RNase H, which is specific for RNA–DNA duplexes, also increased the mobility of the ^{32}P-labeled products, providing evidence that the template RNA is base paired to DNA (Figure 4A). Unexpectedly, however, the predominant RNase H digestion product migrated more slowly than that obtained with RNase A, and the extent of digestion was not increased at higher RNase H concentrations (data not shown). Possible explanations are that some portion of the RNA template is associated with the plasmid via an RNase H–resistant structure (e.g., an R loop or an RNA–DNA triplex) or that RNase H digestion was obstructed by the highly structured intron RNA. Finally, the ^{32}P-labeled products were completely sensitive to DNase digestion, as expected (Figure 4A).

To test whether the nascent ^{32}P-labeled DNA is duplexed to the RNA template, the plasmid products were digested sequentially with RNase A and S_1 nuclease, which is specific for single-stranded nucleic acids. As shown in Figure 4B, S_1 nuclease digestion by itself increased the mobility of the ^{32}P-labeled products to that of linear plasmid, presumably reflecting removal of unpaired portions of the RNA template, but did not affect the intensity of the labeled band. By contrast, the labeled cDNA became sensitive to S_1 nuclease after pretreatment with RNase A. These findings provide evidence that the nascent DNA is base paired to the template RNA, as expected for target DNA–primed reverse transcription.

cDNA Synthesis Occurs at a Double-Strand Break in the Recipient DNA

To localize the site of cDNA synthesis at a nick or double-strand break in the recipient plasmid, we carried out the experiment shown in Figure 4C. In this experiment, the ^{32}P-labeled products were digested by RNase A and restriction enzymes that cleave at a single site in the target plasmid (see map in Figure 4D). If the cDNA is synthesized at a nick, each digest should yield a ^{32}P-labeled band corre-

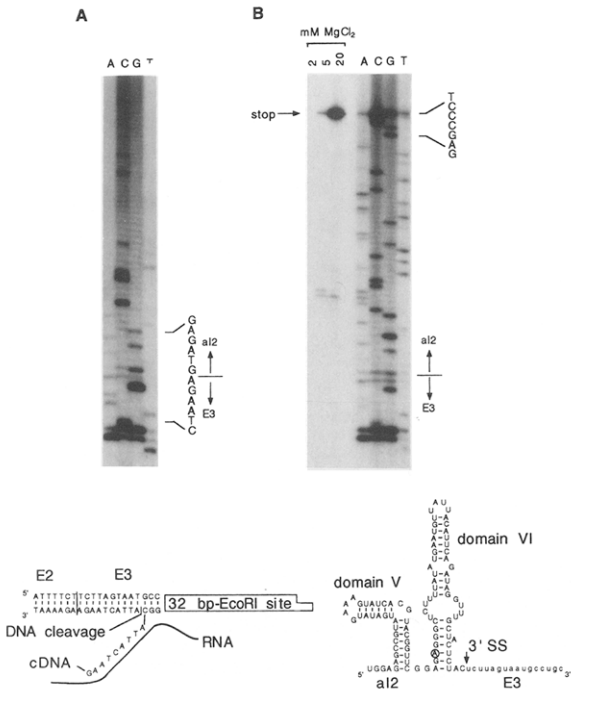

Figure 5. Dideoxy Sequencing of the Nascent cDNA

^{32}P-labeled cDNAs were synthesized by incubating wild-type 1^+2^+ mtRNP particles with plasmid pE2E3 at 20 mM $MgCl_2$ and pH 7.5 in the presence of dideoxynucleotides to generate sequencing ladders. The products were digested with EcoRI and resolved in a 6% polyacrylamide gel. (A) and (B) show reactions with ddNTP to dNTP ratios of 100 μM to 10 μM and 50 μM to 50 μM, respectively. (B) also shows reactions at 2, 5, and 20 mM Mg^{2+} in the absence of ddNTPs. The schematics below show the sequence of the nascent cDNA (left) and the secondary structure at the 3′ end of al2 (right). The circled nucleotide (position −51) indicates the stop site for cDNAs synthesized at the higher Mg^{2+} concentrations.

sponding to monomer-sized plasmid. However, if the cDNA is synthesized at a double-strand break, then the size of the labeled fragment will vary, depending on the distance between the double-strand break and the restriction site. Figure 4C shows that each restriction digest gave a single predominant ^{32}P-labeled fragment of different size, indicating that cDNA synthesis occurs at a double-strand break. From the sizes of the fragments, we infer that the double-strand break is near the E2–E3 junction and that the cDNAs are added to the 3′ end of the antisense (i.e., transcribed) strand, as expected for a reaction related to intron mobility. Time course experiments using higher amounts of labeled nucleotide to detect incorporation at short timepoints failed to detect cDNA synthesis on nicked plasmid prior to the double-strand break (data not shown), in contrast with the situation for the R2Bm RT (Luan et al., 1993).

Dideoxy Sequencing of the Nascent cDNA

To identify the ^{32}P-labeled cDNA product, dideoxynucleotides were included during cDNA synthesis to generate a sequencing ladder of the nascent cDNA (Figure 5). The target DNA–primed reverse transcription reaction was carried out at 20 mM $MgCl_2$ to enhance labeling, and two different proportions of ddNTPs to dNTPs were used to optimize the reading of sequence from different regions. After the reaction, the ^{32}P-labeled plasmid was cleaved at the EcoRI site 35 nt from the cDNA initiation site (see schematic in Figure 5), and the products were analyzed on sequencing gels. The sequence ladders show that cDNA synthesis is initiated just downstream of the intron in exon 3 (Figure 5A) and extends into intron domain VI (Figure 5B). In a related experiment, by analyzing short cDNAs labeled with different [^{32}P]dNTPs and terminated with different ddNTPs, the first nucleotide incorporated was identified as the A residue 10 nt downstream of the intron insertion site (position +10 of exon 3; data not shown).

We noted previously that cDNAs synthesized in reaction medium containing >5 mM Mg^{2+} are shorter than those synthesized at 2 mM Mg^{2+} (see Figure 3). Figure 5B shows that most of the cDNAs synthesized at 5 and 20 mM Mg^{2+} end abruptly at position −51 of al2, and this is true both in the sequencing ladders and in separate cDNA synthesis reactions at 5 and 20 mM Mg^{2+} in the absence of ddNTPs. The truncation of the cDNAs could reflect either site-specific cleavage or termination of cDNA synthesis at position −51, perhaps owing to an impassable secondary structure beginning at domain V of the intron (see schematic, Figure 5, bottom).

Detection of DNA Endonuclease Activity and Mapping of Cleavage Sites

The above results indicate that reverse transcription is primed by the 3′ end of the antisense strand at a double-strand break in the recipient DNA. To assay the DNA endonuclease responsible for the double-strand break directly, we carried out the experiment shown in Figure 6. In this experiment, target DNA substrates of about 200 bp were generated from pE2E3 by polymerase chain reaction (PCR) with different 5′ end–labeled primers to label separately each of the DNA strands. The target DNAs were then incubated with mtRNP particles from different strains, and the resulting cleavages were located by alignment with sequencing ladders. The reactions were carried out at 20 mM $MgCl_2$, found in separate experiments to be optimal for the DNA endonuclease activity (data not shown). Figure 6 shows that wild-type 1^+2^+ and 1^02^{+t} mtRNP particles have readily detectable DNA endonuclease activity that cleaves each strand of the recipient DNA at a specific site. The antisense strand is cleaved at position +10 of exon 3, exactly where expected from the cDNA initiation site, and the sense strand is cleaved precisely at the exon 2–exon 3 junction. The endonuclease activity was not detected with boiled wild-type RNP particles or with RNP particles from the 1^02^0 strain that lacks al2. When dNTPs were added to support cDNA synthesis, the endonuclease activity was unaffected, except that some proportion of the antisense strand fragments were elongated as expected (Figure 6). Primer extension mapping of the cleavage sites from the opposite direction confirmed that the antisense strand cleavage site is not affected by dNTPs (data not shown).

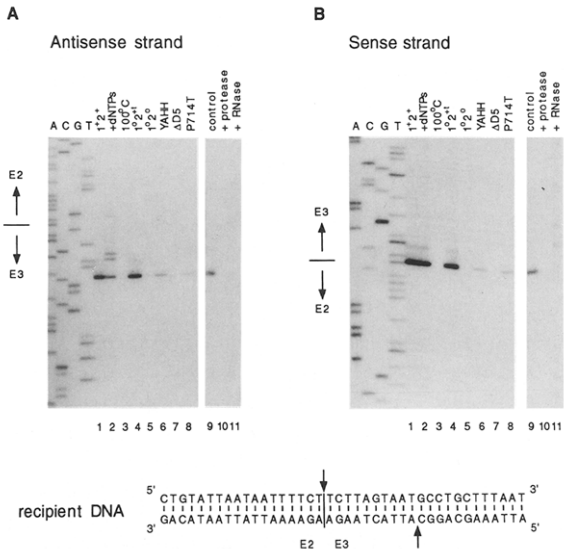

Figure 6. Mapping of DNA Endonuclease Cleavage Sites in the Target DNA

DNA substrates containing the al2 homing site were synthesized from pE2E3 by PCR using 5′ end-labeled primers to label separately the antisense and sense strands (see Experimental Procedures). The target DNAs were incubated with mtRNP particles from the strains indicated below in reaction medium containing 20 mM Mg^{2+}, and the cleavage products were analyzed in a 6% polyacrylamide, 8 M urea gel alongside sequencing ladders generated from pE2E3 with the same 5′ end-labeled primers. Lane 1, wild-type 161 ($1^{+}2^{+}$); lane 2, $1^{+}2^{+}$ with 0.2 mM dNTPs to support cDNA synthesis during the incubation; lane 3, $1^{+}2^{+}$ preincubated at 100°C for 5 min; lane 4, $1^{0}2^{+}$; lane 5, $1^{0}2^{0}$; lane 6, $1^{0}2^{YAHH}$ (YAHH); lane 7, $1^{0}2^{\Delta D5}$ (ΔD5); lane 8, $1^{0}2^{P714T}$ (P714T); Lanes 9–11, $1^{+}2^{+}$ mtRNP particles preincubated for 2 min in the absence (control) or presence of proteinase K (1 μg, 37°C) or RNase A (1 μg, 37°C). The reactions for lanes 9–11 were in the presence of 7 μg of pBluescript KS(+) to compete for nonspecific nuclease activity released by RNase digestion of the RNP particles. The diagram below shows the sequence at the al2 homing site with the cleavage sites indicated by arrows.

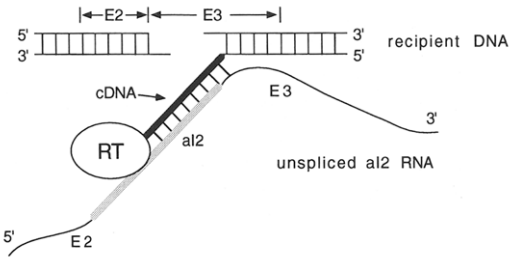

Figure 7. Retrotransposition Mechanism of the Group II Intron al2

Retrotransposition is initiated by a site-specific DNA endonuclease activity that makes a double-strand break at the al2 homing site in the recipient DNA. The 3′ OH of the antisense strand cleaved at position +10 of exon 3 serves as the primer for reverse transcription of *COX1* pre-mRNA containing the al2 intron (stippled). Reverse transcription results in a cDNA (bold) that begins in exon 3 and extends through al2 into the upstream exons. Because of homology with the upstream exons, the cDNA can replace the corresponding region of the recipient DNA by a gap-repair process leading to transfer of the intron with coconversion of flanking exon sequences. Second-strand synthesis primed by the sense strand of the recipient DNA may be carried out by either the al2 RT or yeast mtDNA polymerase.

DNA Endonuclease Activity in Mutant Strains

Figure 6 also shows DNA endonuclease assays for the three previously described al2 mutants. First, the data show that mtRNP particles from the $1^{0}2^{YAHH}$ mutant, which lack detectable RT activity, retain DNA endonuclease activity that accurately cleaves both strands of the recipient DNA. Although the extents of cleavage appear reduced compared with wild-type RNP particles, this finding shows that endonuclease activity can be genetically separated from the RT activity of the al2 protein.

Second, mtRNP particles from the Zn domain mutant $1^{0}2^{P714T}$ have reduced DNA endonuclease activity compared with wild-type mtRNP particles. In quantitative assays normalized by either OD_{260} or soluble al2 RT activity, the cleavage activities for the antisense and sense strands in the mutant were 6% and 25%, respectively, of $1^{+}2^{+}$ RNP particles (data not shown). The DNA endonuclease activities in both wild type and the mutant fall off rapidly at 2–5 mM Mg^{2+} and could not be compared directly under these conditions. However, the finding that the $1^{0}2^{P714T}$ mutant shows little if any target-primed DNA synthesis at 2 mM Mg^{2+} (Figure 1; data not shown) likely reflects that the mutant is unable to cleave the target plasmid under these conditions. The low antisense strand cleavage activity in the $1^{0}2^{P714T}$ mutant may account for the impaired mobility of al2 in that strain and is consistent with the hypothesis that endonuclease activity is associated with the Zn domain of the al2 protein.

Finally, the splicing-defective mutant $1^{+}2^{\Delta D5}$ shows no detectable cleavage of either DNA strand. Since the mtRNP particles from the $1^{+}2^{\Delta D5}$ strain contain elevated amounts of the 62 kDa al2 protein that retains RT activity (data not shown), this finding suggests that the splicing or structural integrity of al2 is also required for the endonuclease activity. Supporting this inference, Figure 6 shows that the endonuclease activity for both strands is inhibited by pretreatment of the wild-type RNP particles with either proteinase K or RNase A. Taken together, these findings indicate that the DNA endonuclease activity is associated with an RNP complex containing both the al2-encoded protein and al2 RNA.

Discussion

Our results indicate that group II intron retrotransposition proceeds via the mechanism illustrated in Figure 7. The process is initiated by a site-specific DNA endonuclease activity, which generates a double-strand break in the recipient DNA. The sense strand is cleaved at the junction between exons 2 and 3, and the antisense strand is cleaved at position +10 of exon 3. The 3′ end of the antisense strand cleaved in exon 3 is used as a primer for reverse transcription of the *COX1* pre-mRNA of the donor, leading to synthesis of a cDNA that begins in exon 3 and extends through the intron into the upstream exons. The priming event may involve formation of an R loop or triplex between exon 3 sequences in the recipient DNA and the *COX1* pre-mRNA of the donor. Homing is presumably com-

pleted by the replacement of upstream recipient sequences by the cDNA, either before or after second-strand synthesis. This model accounts for the site specificity of homing, its dependence on the al2 RT activity, and the coconversion of the intron with flanking exon sequences.

Consistent with the phylogenetic relationship of their RTs, the group II intron retrotransposition mechanism is analogous to that used by non-LTR retrotransposons, particularly the well-characterized R2Bm element (Eickbush, 1992; Luan et al., 1993). The latter also encodes a RT having a site-specific endonuclease activity involved in mobility. However, the R2Bm-encoded protein cleaves the recipient DNA directly at the insertion site of the element, and reverse transcription is initiated at the 3′ end of the RNA encoded by the element (Luan et al., 1993). In contrast with group II intron mobility, this process results in a 2 bp deletion of target sequences, reflecting that the endonuclease makes a staggered cut in the two strands and that the 5′ overhangs are removed by nuclease digestion prior to integration. For other non-LTR elements, such as LINEs, retrotransposition results in short target site duplications, presumably reflecting that the single-stranded tails at the target site are not removed prior to integration (Eickbush, 1992).

In contrast with the R2Bm mechanism, in which reverse transcription in vitro occurs on nicked recipient DNA prior to the second-strand cleavage (Luan et al., 1993), target DNA–primed reverse transcription by the al2 RT appears to occur predominantly at a double-strand break. Although we cannot exclude that the group II intron RT initiates on nicked recipient DNA in vivo, this possibility seems less likely since we could detect no cDNA synthesis on nicked recipient DNA in vitro. In addition, time course experiments have shown that the al2 endonuclease cleaves the sense strand of the recipient DNA more rapidly than it cleaves the antisense strand used as primer (data not shown). This situation is exactly opposite that for the R2Bm RT (Luan et al., 1993) and suggests why cDNA synthesis by the group II intron RT may not occur until after a double-strand break has been made.

Our previous analysis of missense mutants of the al2 ORF suggested that efficient homing requires both the al2 RT activity and a suspected DNA endonuclease activity associated with the Zn domain (Moran et al., 1995). The present results provide direct evidence for this endonuclease activity and show that it specifically cleaves recipient *COX1* alleles near the al2 homing site to generate a primer for cDNA synthesis. The finding that target DNA–primed reverse transcription does not occur with plasmids containing only exon 3 or donor alleles in which exons 2 and 3 are separated by al2 suggests that the endonuclease recognizes features present only when exons 2 and 3 are adjacent. The endonuclease activity appears to be associated with the Zn domain of the al2 protein and is genetically separable from the RT activity. The finding that the YAHH mutation in the RT domain of the al2 protein eliminates RT activity, but not DNA endonuclease activity supports our previous suggestion that the residual intron homing observed in that strain results from a double-strand break repair mechanism similar to that used by mobile group I introns (Moran et al., 1995). As expected from this interpretation, the Zn domain mutant $1^{0}2^{P714T}$ is almost completely deficient in mobility, suggesting that the same endonuclease activity can promote mobility by both the RT-dependent and RT-independent mechanisms (Moran et al., 1995).

Sainsard-Chanet et al. (1994) previously detected in vivo double-strand breaks at the 5′ splice sites of two RT-encoding group II introns in Podospora mtDNA and speculated that these might involve an endonuclease that functions in group II intron homing via a target DNA–primed reverse transcription mechanism. However, the relationship of these cleavages to intron homing is not clear, since we find that intron-containing alleles are not substrates for target DNA–primed reverse transcription in vitro.

Following cleavage of the recipient DNA in exon 3, the al2 RT initiates cDNA synthesis with high specificity at position +10 of exon 3. The initiation of cDNA synthesis at this position in unspliced *COX1* pre-mRNA explains the previous observation that efficient coconversion of exon sequences extends farther upstream in exon 1 than it does downstream in exon 3 (Lazowska et al., 1994; Moran et al., 1995). Among the exon 3 markers studied by us, a nucleotide change at exon 3 position +23 coconverted with al2 about 60% of the time, whereas a nucleotide change at exon 3 position +34 showed no detectable coconversion (Moran et al., 1995). The coconversion at the +23 position, 13 bp downstream of the in vitro initiation site, suggests that the priming strand may be digested back for some distance prior to the initiation of reverse transcription in vivo. On the other hand, the lack of detectable coconversion at position +34 indicates either that the priming strand is rarely digested back this far or that such events rarely lead to intron insertion. In fact, exon 3 is only 35 bp long. If R loop or triplex formation within exon 3 is important for homing, then extensive digestion from the cut site should block the process. An alternate possibility is that the coconversion at the +23 position in exon 3 reflects that some mobility in vivo occurs independently of reverse transcription by a double-strand break repair mechanism mediated by the al2 endonuclease activity (see Moran et al., 1995).

Several findings indicate that the al2 RT binds specifically near the 3′ end of the intron in unspliced pre-mRNA, where it is positioned to initiate reverse transcription once the primer is formed by the action of the endonuclease. Thus, the Zn domain mutant $1^{0}2^{P714T}$, which is deficient in DNA endonuclease activity, has elevated RT activity with endogenous templates and synthesizes cDNAs beginning at scattered locations in exon 3 and in domain VI of the intron, presumably by an alternate mechanism that does not involve the exon 3 DNA primer (Kennell et al., 1993). Further, this mutant splices al2 normally, suggesting that the specific binding of the al2 protein to the intron RNA is not impaired. Similarly, the splicing-defective mutant $1^{+}2^{\Delta D5}$ has no detectable DNA endonuclease activity, but still has high endogenous RT activity and can initiate on *COX1* pre-mRNA to synthesize cDNAs containing al2

(Moran et al., 1995; J. C. Kennell and A. M. L., unpublished data). It may be pertinent that the Mauriceville plasmid RT, which is related to the group II intron RTs, can initiate cDNA synthesis by multiple mechanisms, including de novo initiation or by using a DNA or RNA primer (Wang and Lambowitz, 1993).

Remarkably, our results provide evidence that the DNA endonuclease activity that initiates homing requires al2 RNA, as well as the al2-encoded protein. Genetic studies indicate that the endonuclease activity is inhibited by mutations in both the al2 protein ($1^0 2^{P714T}$) and al2 RNA ($1^+ 2^{\Delta D5}$), and biochemical studies show that the activity is sensitive to both proteinase and RNase. Notably, the $1^+ 2^{\Delta D5}$ mutant, which has a deletion of intron domain V required for catalytic activity in splicing, continues to synthesize active al2 RT, but has no detectable endonuclease activity. Since group II intron RNAs have been shown to cleave DNA site specifically (Mörl et al., 1992), the al2 RNA could in principle be either a catalytic component or cofactor of the endonuclease (Saldanha et al., 1993; Belfort, 1993). The cleavage at the exon 2–exon 3 junction of the sense strand is, in fact, exactly as expected for a group II intron ribozyme activity. On the other hand, a cofactor role for the RNA is favored by the findings that the Zn domain of the al2 protein has amino acid sequence similarity to known DNA endonucleases (Gorbalenya, 1994; Shub et al., 1994) and that the antisense strand cleavage in exon 3 is not at a site expected for any known group II intron ribozyme activity. A requirement for an intron RNA cofactor would be reminiscent of the situation for the R2Bm RT, which efficiently cleaves one strand of the target DNA, but requires an RNA cofactor to cleave the opposite strand (Luan et al., 1993). For the al2 RT, the RNA cofactor could be either the excised intron or the unspliced intron in the pre-mRNA template. A requirement for splicing-competent intron RNA ensures that only functional introns will be mobile, thereby minimally impairing host gene expression.

The presence of RT-encoding group II introns in bacteria as well as in organelles that evolved from endosymbiotic bacteria (Ferat and Michel, 1993) suggests that mobile group II introns predated nuclear non-LTR retrotransposons. Cavalier-Smith (1991) and Palmer and Logsdon (1991) proposed that nuclear spliceosomal introns evolved from group II introns that migrated from organelles to the nucleus in early eukaryotes. This hypothesis is based on the well-documented transfer of mitochondrial and chloroplast DNA to the nucleus (Nugent and Palmer, 1991) and on the apparent lack of spliceosomal introns in amitochondrial eukaryotes, such as Giardia. The similarity in retrotransposition mechanisms found in this study raises the possibility that mobile group II introns were not only the progenitors of nuclear pre-mRNA introns but also of nuclear non-LTR retrotransposons. Group II introns that inserted into genes may have been forced to maintain splicing competence and evolve as introns, whereas those inserted into nonfunctional regions could lose splicing competence and evolve as mobile elements. Since many nuclear non-LTR retrotransposons appear to lack endonuclease domains required for site-specific insertion (Eickbush, 1992), it is necessary to postulate either that group II introns acquired this activity subsequently or that it was lost by nuclear non-LTR retrotransposons. The suspected endonuclease domain of the R2Bm element, which is specific for multicopy rRNA genes, is located upstream of the RT domain (Luan et al., 1993) and may have been acquired independently of that associated with group II intron RTs.

Finally, we note that the ability of group II intron RTs to use the 3′ end of genomic DNA to prime reverse transcription is similar to that of telomerases, specialized RTs that add short DNA repeats to the 3′ ends of chromosomes (Blackburn, 1991). Telomerases use the 3′ end of chromosomal DNA as a primer for reverse transcription of an integral RNA template encoding the telomeric repeats. The analogy between the telomerase mechanism and target DNA–primed reverse transcription is emphasized by the finding that Drosophila lacks a conventional telomerase, and this function is fulfilled directly by non-LTR retrotransposons (HeT-A and TART) that use 3′ ends of chromosomal DNA to prime reverse transcription of the RNA of the element (see Levis et al., 1993). An intriguing possibility is that telomerases, which are required for the maintenance of eukaryotic chromosomes, were also derived from an RT originally associated with mobile group II introns in early eukaryotes.

Experimental Procedures

Yeast Strains and Growth Conditions

The yeast strains used in this study were described in Kennell et al. (1993) and Moran et al. (1995). The intron composition of each strain is denoted by a convention in which a superscripted plus indicates the presence of wild-type al1 or al2, a superscripted zero indicates the absence of the intron, and other superscripts refer to specific alleles. The wild-type 1^+2^+ strain is ID41-6/161 *MATa ade1 lys1* (denoted 161). $1^0 2^{+t}$ lacks al1 and contains al2 derived from wild-type 161. $1^+ 2^0$ lacks al2 and contains al1 derived from wild-type 161. The $1^0 2^0$ strain (GII-O) is the standard recipient strain used to test homing of al1 and al2 in crosses (Moran et al., 1995). $1^0 2^{YAHH}$ lacks al1 and has the mutation YADD→YAHH in the RT domain of the al2 protein. $1^0 2^{P714T}$ lacks al1 and has a mobility-deficient al2 allele carrying the mutation P714T in the Zn domain of the al2 protein. $1^+ 2^{\Delta D5}$ contains a splicing-defective al2 allele with a deletion of intron domain V. Yeast strains were grown in liquid culture as described (Kennell et al., 1993), except that the carbon source for mit^+ strains was either 3% glycerol or 2% raffinose. Cells grown in raffinose were routinely tested for mitochondrial function by plating on glycerol and glucose media.

Recombinant Plasmids

Plasmids pJVM4, pJVM32, pJVM139, pJVM159, and pMTV contain different segments of the yeast *COX1* gene cloned in pBluescript KS(+) or pBluescribe (+) vectors (Kennell et al., 1993; see Figure 2 for diagram of plasmid inserts).

pHG1 was obtained from pJVM159 by subcloning the 1.9 kb ClaI–BamHI fragment into pBluescript KS(+). The insert begins in al1 and extends through al3.

pSZD1 was derived from pJVM4 by deleting the al2 ORF from positions 3247–4797. To construct pSZD1, the 5′ portion of the pJVM4 insert was amplified by PCR using the M13 reverse primer and the oligonucleotide 5′GAAGATCTCTCGGAAAAATCCGTAG, which is complementary to al2 positions 3230–3246 (numbered according to Bonitz et al. [1980]) with an added BglII site. The PCR fragment was cut with ClaI and BglII and cloned between the ClaI site (polylinker) and BglII site at al2 position 4798 of pJVM4.

Plasmid pE2E3 contains a 71 bp insert consisting of *COX1* exons

2 and 3 cloned in the SmaI site of pBluescript KS(+). The insert was generated from GII-0 mtDNA by PCR using the primers 5′-TTTTAGTAGCTGGTCATGCTGTATT and 5′-ACCAAAACCTCCTATTAAAGCAGGC. The insert differs from wild-type 161 sequence at three positions: T to C at position 10 of exon 2, G to A at position 29 of exon 2, and T to A at position 23 of exon 3.

Preparation of Mitochondria and mtRNP Particles

Mitochondria and mtRNP particles were isolated as described (Kennell et al., 1993). The RNP particle pellet was resuspended in 10 mM Tris–HCl (pH 8.0), 1 mM DTT and stored at −70°C.

In Vitro Assay of Target DNA-Primed Reverse Transcription

Target DNA–primed reverse transcription was assayed in 10 μl of reaction medium containing 1 μg of recipient plasmid DNA, 0.025 U of mtRNP particles (OD_{260}), 0.2 mM each of dATP, dGTP, and dTTP, 10 μCi of [α-^{32}P]dCTP (3,000 Ci/mmole; DuPont–New England Nuclear, Boston, MA), 100 mM KCl, and 5 mM dithiothreitol (DTT), with different concentrations of $MgCl_2$, and 50 mM Tris–HCl at pH 7.5 or 8.5, as indicated for individual experiments. The reactions were initiated by addition of RNP particles, incubated for 10 min at 37°C, and chased with 0.2 mM dCTP for another 10 min. After the chase period, the reactions were terminated by extraction with phenol–CIA (phenol:chloroform:isoamyl alcohol, 25:24:1) in the presence of 0.3 M sodium acetate (pH 7.8) and 5 μg of Escherichia coli tRNA carrier (Sigma, St. Louis, MO). Products were ethanol precipitated twice and resolved in 1% agarose gels containing 90 mM Tris–borate (pH 8.3), 2 mM EDTA, and 0.05% ethidium bromide. The gels were dried and autoradiographed.

Optimization experiments showed that reverse transcription is more processive at 2 mM Mg^{2+} than at higher Mg^{2+} concentrations, whereas the site-specific DNA endonuclease activity required to generate the primer is optimal at higher Mg^{2+} concentrations. ^{32}P incorporation into the recipient plasmid has a temperature optimum of 37°C–42°C and a broad KCl optimum between 50 and 150 mM, which varies somewhat with Mg^{2+} concentration and pH. In reaction medium containing 100 mM KCl and 50 mM Tris–HCl, the pH optimum is 8.5 at 2 mM Mg^{2+} and 7.5 at 5 mM Mg^{2+}. Based on these results, we used reaction medium containing 100 mM KCl, 2 mM $MgCl_2$, 50 mM Tris–HCl (pH 8.5), and 5 mM DTT for experiments requiring synthesis of elongated cDNAs and reaction medium containing 100 mM KCl, 5 mM $MgCl_2$, 50 mM Tris–HCl (pH 7.5), and 5 mM DTT for experiments requiring maximal labeling of cDNAs or for endonuclease assays.

Nuclease Digestion of Putative Mobility Products

The ^{32}P-labeled plasmid products resulting from target DNA–primed reverse transcription reactions were characterized by digestion with various nucleases. RNase A digestion was for 15 min at 37°C in 50 μl of low salt buffer containing 0.1 μg of RNase A (Sigma), 10 mM Tris–HCl (pH 8.0), and 1 mM EDTA. RNase H digestion was for 30 min at 37°C in 50 μl of reaction medium containing 2.7 U of RNase H (Life Technologies, Incorporated, Gaithersburg, MD), 100 mM KCl, 10 mM $MgCl_2$, 20 mM Tris–HCl (pH 7.5), and 0.1 mM DTT. DNase I digestion was for 30 min at 37°C in 50 μl of reaction medium containing 7.5 U of DNase I (Pharmacia, Piscataway, NJ), 100 mM NaOAc (pH 4.6), and 5 mM $MgCl_2$. For sequential RNase A and S_1 nuclease digestion (Figure 4B), the RNase A digestion was carried out as above, except that the reaction medium contained salmon sperm DNA carrier (2 μg of dsDNA and 1 μg of ssDNA). After extraction with phenol–CIA and ethanol precipitation, the S_1 nuclease digestion was for 30 min at 25°C in 50 μl of reaction medium containing 8 U of S_1 nuclease (Pharmacia), 30 mM NaOAc (pH 4.6), 50 mM NaCl, 1 mM $ZnCl_2$, and the carrier DNA. In Figure 4C, the ^{32}P-labeled plasmid products were digested for 1 hr at 37°C with 0.1 μg of RNase A plus 10 U of restriction enzyme (NotI, ScaI, AlwNI, or EcoRI; Life Technologies, Incorporated) in 300 μl of the corresponding buffer (also obtained from the manufacturer). Nuclease digestion products were extracted with phenol–CIA, ethanol-precipitated, and analyzed by electrophoresis on 1% agarose gels.

Dideoxy Sequencing of Nascent cDNA

For direct dideoxy sequencing, target DNA–primed reverse transcription reactions were carried out in 10 μl of reaction medium containing 0.025 U of 1^+2^+ mtRNP particles (OD_{260}), 1 μg of recipient plasmid pE2E3, 100 mM KCl, 20 mM $MgCl_2$, 50 mM Tris–HCl (pH 7.5), and 5 mM DTT, plus 50 μCi of [α-^{32}P]dTTP (3,000 Ci/mmole; DuPont–New England Nuclear) for the A, C, and G lanes, and 50 μCi of [α-^{32}P]dATP (3,000 Ci/mmole; DuPont–New England Nuclear) for the T lanes. One set of reactions used a ddNTP to dNTP ratio of 100 μM to 10 μM, and a second set used a ratio of 50 μM to 50 μM. The two remaining dNTPs were 0.2 mM. The reactions were incubated for 10 min at 37°C and then chased for 10 min with 0.2 mM of the dNTP corresponding to the radiolabel. The reactions were terminated by extraction with phenol–CIA in the presence of 0.3 M NaOAc and 5 μg of E. coli tRNA carrier, followed by ethanol precipitation. The products were then digested with 10 U of EcoRI, 1 U of alkaline phosphatase (Boehringer Mannheim, Indianapolis, IN), and 0.1 μg of RNase A for 1 hr at 37°C. Sequencing ladders were resolved in a 6% polyacrylamide, 8 M urea gel, which was dried and autoradiographed.

Assay of DNA Endonuclease Activity

DNA substrates for endonuclease assays were generated from pE2E3 by PCR using 5′ end–labeled primers to label separately the antisense and sense strands. The antisense strand substrate (216 bp) was synthesized by using the M13 forward primer with the 5′ end–labeled primer KS (5′-TCGAGGTCGACGGTATC), which is complementary to a sequence in the polylinker. The sense strand substrate (224 bp) was synthesized by using the M13 reverse primer with the 5′ end–labeled primer SK (5′-CGCTCTAGAACTAGTGGATC), complementary to a sequence in the opposite polylinker. The primers (0.2 μg) were radiolabeled by using T4 polynucleotide kinase (New England Biolabs, Beverly, MA) and 150 μCi of [γ-^{32}P]ATP (3,000 Ci/mmole; DuPont–New England Nuclear) (Sambrook et al., 1989). Following PCR, the labeled substrate DNAs were purified in a 1.5% agarose gel, extracted with phenol–CIA, and ethanol precipitated. DNA endonuclease activity was assayed by incubating 50 fmole (~7.3 ng) of the ^{32}P-labeled DNA substrate with 0.025 U of mtRNP particles (OD_{260}) in 10 μl of reaction medium containing 100 mM KCl, 20 mM $MgCl_2$, 50 mM Tris–HCl (pH 7.5), and 5 mM DTT. Reactions were initiated by addition of RNP particles, incubated for 20 min at 37°C, and terminated by phenol–CIA extraction in the presence of 0.3 M NaOAc and 2 μg of single-stranded salmon sperm DNA, followed by ethanol precipitation. Products were analyzed in a 6% polyacrylamide, 8 M urea gel, alongside sequencing ladders generated from pE2E3 with the corresponding 5′ end–labeled primer.

Acknowledgments

We thank Mr. James Williams for technical assistance. This work was supported by National Institutes of Health grant GM37949 to A. M. L. and GM31480 to P. S. P.

Received April 27, 1995; revised June 15, 1995.

References

Belfort, M. (1993). An expanding universe of introns. Science *262*, 1009–1010.

Blackburn, E. H. (1991). Structure and function of telomeres. Nature *350*, 569–573.

Bonitz, S. G., Coruzzi, G., Thalenfeld, B. E., Tzagoloff, A., and Macino, G. (1980). Assembly of the mitochondrial membrane system: structure and nucleotide sequence of the gene coding for subunit 1 of yeast cytochrome oxidase. J. Biol. Chem. *255*, 11927–11941.

Carignani, G., Groudinsky, O., Frezza, D., Schiavon, E., Bergantino, E., and Slonimski, P. P. (1983). An mRNA maturase is encoded by the first intron of the mitochondrial gene for the subunit I of cytochrome oxidase in S. cerevisiae. Cell *35*, 733–742.

Cavalier-Smith, T. (1991). Intron phylogeny: a new hypothesis. Trends Genet. *7*, 145–148.

Doolittle, R. F., Feng, D.-F., Johnson, M. S., and McClure, M. A. (1989). Origins and evolutionary relationships of retroviruses. Quart. Rev. Biol. *64*, 1–30.

Eickbush, T. H. (1992). Transposing without ends: the non-LTR retrotransposable elements. New Biol. *4*, 430–440.

Eickbush, T. H. (1994). Origin and evolutionary relationships of retroelements. In The Evolutionary Biology of Viruses, S. S. Morse, ed. (New York: Raven Press), pp. 121–157.

Ferat, J. L., and Michel, F. (1993). Group II self-splicing introns in bacteria. Nature *364*, 358–361.

Gorbalenya, A. E. (1994). Self-splicing group I and group II introns encode homologous (putative) DNA endonucleases of a new family. Protein Sci. *3*, 1117–1120.

Kennell, J. C., Moran, J. V., Perlman, P. S., Butow, R. A., and Lambowitz, A. M. (1993). Reverse transcriptase activity associated with maturase-encoding group II introns in yeast mitochondria. Cell *73*, 133–146.

Lambowitz, A. M., and Belfort, M. (1993). Introns as mobile genetic elements. Annu. Rev. Biochem. *62*, 587–622.

Lazowska, J., Meunier, B., and Macadre, C. (1994). Homing of a group II intron in yeast mitochondrial DNA is accompanied by unidirectional co-conversion of upstream-located markers. EMBO J. *13*, 4963–4972.

Levis, R. W., Ganesan, R., Houtchens, K., Tolar, L. A., and Sheen, F. (1993). Transposons in place of telomeric repeats at a Drosophila telomere. Cell *75*, 1083–1093.

Luan, D. D., Korman, M. H., Jakubczak, J. L., and Eickbush, T. H. (1993). Reverse transcription of R2Bm RNA is primed by a nick at the chromosomal target site: a mechanism for non-LTR retrotransposition. Cell *72*, 595–605.

Meunier, B., Tian, G.-L., Macadre, C., Slonimski, P. P., and Lazowska, J. (1990). Group II introns transpose in yeast mitochondria. In Structure, Function and Biogenesis of Energy Transfer Systems, E. Quagliariello, S. Papa, F. Palmieri, and C. Saccone, eds. (Amsterdam: Elsevier Scientific Publishing Company), pp. 169–174.

Michel, F., and Lang, B. F. (1985). Mitochondrial class II introns encode proteins related to the reverse transcriptases of retroviruses. Nature *316*, 641–643.

Michel, F., Umesono, K., and Ozeki, H. (1989). Comparative and functional anatomy of group II catalytic introns: a review. Gene *82*, 5–30.

Mohr, G., Perlman, P. S., and Lambowitz, A. M. (1993). Evolutionary relationships among group II intron-encoded proteins and identification of a conserved domain that may be related to maturase function. Nucl. Acids Res. *21*, 4991–4997.

Moran, J. V., Mecklenburg, K. L., Sass, P., Belcher, S. M., Mahnke, D., Lewin, A., and Perlman, P. S. (1994). Splicing defective mutants of the *COX1* gene of yeast mitochondrial DNA: initial definition of the maturase domain of the group II intron A12. Nucl. Acids Res. *22*, 2057–2064.

Moran, J. V., Zimmerly, S., Eskes, R., Kennell, J. C., Lambowitz, A. M., Butow, R. A., and Perlman, P. S. (1995). Mobile group II introns of yeast mitochondrial DNA are novel site-specific retroelements. Mol. Cell. Biol. *15*, 2828–2838.

Mörl, M., Niemer, I., and Schmelzer, C. (1992). New reactions catalyzed by a group II intron ribozyme with RNA and DNA substrates. Cell *70*, 803–810.

Mueller, M. W., Allmaier, M., Eskes, R., and Schweyen, R. J. (1993). Transposition of group II intron al1 in yeast and invasion of mitochondrial genes at new locations. Nature *366*, 174–176.

Nugent, J. M., and Palmer, J. D. (1991). RNA-mediated transfer of the gene *coxII* from the mitochondrion to the nucleus during flowering plant evolution. Cell *66*, 473–481.

Palmer, J. D., and Logsdon, J. M., Jr. (1991). The recent origins of introns. Curr. Opin. Genet. Dev. *1*, 470–477.

Sainsard-Chanet, A., Begel, O., and Belcour, L. (1994). DNA double-strand break *in vivo* at the 3′ extremity of exons located upstream of group II introns. J. Mol. Biol. *242*, 630–643.

Saldanha, R., Mohr, G., Belfort, M., and Lambowitz, A. M. (1993). Group I and group II introns. FASEB J. *7*, 15–24.

Sambrook, J., Fritsch, E. F., and Maniatis, T. (1989). Molecular Cloning: A Laboratory Manual (Cold Spring Harbor, New York: Cold Spring Harbor Laboratory Press).

Shub, D. A., Goodrich-Blair, H., and Eddy, S. R. (1994). Amino acid sequence motif of group I intron endonucleases is conserved in open reading frames of group II introns. Trends Biochem. Sci. *19*, 402–404.

Wang, H., and Lambowitz, A. M. (1993). The Mauriceville plasmid reverse transcriptase can initiate cDNA synthesis de novo and may be related to reverse transcriptase and DNA polymerase progenitor. Cell *75*, 1071–1081.

Xiong, Y., and Eickbush, T. H. (1990). Origin and evolution of retroelements based upon their reverse transcriptase sequences. EMBO J. *9*, 3353–3362.